Int. J. Solids Structures Vol. 30, No. 11, pp. 1473–1489, 1993
Printed in Great Britain

0020–7683/93 $6.00+ .00

MULTIPLE VOID–CRACK INTERACTION

K. X. HU, A. CHANDRA and Y. HUANG
Department of Aerospace and Mechanical Engineering, The University of Arizona, Tucson, AZ 85721, U.S.A.

(*Received* 16 *March* 1992; *in revised form* 5 *November* 1992)

Abstract—This paper presents a method for fracture analysis of a general two-dimensional system containing multiple holes, or voids, and cracks. The superposition technique is used to break the problem into a number of single-hole and single-crack problems. Each hole problem is modeled using the method of pseudo-tractions, and each crack problem is modeled by a distribution of dislocations. An integral equation approach is developed, based on two types of fundamental solutions, one due to point loads in a solid with a hole and the other due to point dislocations in an infinite elastic body. The resulting integral equations present Cauchy-type singularities only on the crack part of the multiple hole–crack problem. The results in terms of stress intensity factors (SIFs) are presented for a variety of hole-and-crack arrangements, relative sizes of cracks and holes, spacings and crack orientations. The amplification and retardation effects on SIFs are investigated. It is found that the hole–crack arrangements have significant effects on the nature of the amplification or retardation. In the fractured porous elastic medium (modeled as a crack surrounded by holes), amplification or retardation can occur, depending on the relative size of the holes and cracks and the spacing between them. Very strong retardation exists as the spacing becomes small. Some optimal retardations (void toughening) are achieved by adjusting the geometry parameters. An array of periodical crack–hole structure is examined as a numerical example.

1. INTRODUCTION

Many brittle materials, such as rocks, ceramics and intermetallics, have a pre-existing subscale flaw structure in the form of voids, cracks, and other inclusions. Accurate prediction of the explicit fracture response of these materials would require an accurate accounting of the growth of the voids and cracks and their interactions. Many observed nonlinear phenomena in brittle materials are the result of initiation, growth, interaction and coalescence of voids and cracks. For example, the initial stable growth of microcracks is found to be associated with strain-hardening stress–strain behavior, and the interaction and coalescence of cracks are relevant to unstable strain-softening stress–strain behavior (Hallbauer *et al.*, 1973). Both strain-hardening and strain-softening behavior exhibit dilatation as a result of extensible void and crack growth (McMeeking and Evans, 1982; Budiansky *et al.*, 1983). Also, experiments have shown that the average length of the cracks is reduced at higher confining pressures, promoting the transition from brittle to semi-brittle behavior (Fredrich *et al.*, 1989).

Based on microstructure-derived moduli for fractured solids (Budiansky and O'Connell, 1976; Horii and Nemat-Nasser, 1983), various researchers have developed continuum damage micromechanical models for brittle materials (Kachanov, 1982; Sumarac and Krajcinovic, 1987; Ju, 1991). These models are attractive because they express the loss of moduli in terms of evolution of the microstructures and, consequently, they do not involve to-be-determined material parameters. One important aspect of these models is that even though they are based on linear fracture mechanics, nonlinear stress–strain relations can be predicted due to the growth, interaction, and coalescence of the voids and cracks in an otherwise linear-elastic solid (Kemeny and Cook, 1986). Although the quantitative experimental verification of these micromechanical models is extremely complicated, the incorporation of a damage evolution law into the detailed fracture mechanics analysis seems very promising. This will not only provide detailed local behavior, such as stress intensity factors, but also has the potential to obtain the global stress–strain behavior. Using a unit cell approach (Hu *et al.*, 1992; Huang *et al.*, 1992), this may be obtained by modeling only a finite number of defects. Such global stress–strain responses of damaged bodies can be utilized for quantitative verification of various micromechanical models.

This paper focuses on a general approach to such detailed local behavior analysis for systems containing multiple voids and cracks. To simplify the analysis, the voids are assumed to be circular holes and cracks are assumed to be one-dimensional line slits. The problem of cracks extending from the edges of a circular hole was solved by Bowie (1956) using a mapping function method. The hole–crack–hole problem was examined by Newman (1969) using a collocation method. The problem containing holes and/or cracks was studied by Isida and his co-workers [see, for example, Isida (1970a, b, 1973), Isida *et al.* (1985), Isida and Nemat-Nasser (1987), and Isida and Igawa (1991)]. The problems involving cracks and a single circular void, as well as interactions among voids, were also considered by Atkinson (1972), Erdogan *et al.* (1974), and Chen (1984a, b, 1985). The problem involving several cracks has been considered by several researchers and the results can be found in the stress intensity factor handbooks (Sih, 1973; Tada *et al.*, 1985). In recent years, multiple-crack-related micromechanical analysis has become an area of research interest (Horii and Nemat-Nasser, 1985; Kachanov and Montagut, 1986; Rubinstein, 1986, 1990; Chudnovsky *et al.*, 1987a, b; Hori and Nemat-Nasser, 1987; Kachanov, 1987; Hu and Chandra, 1992). Analysis of hole–hole interactions using the pseudo-traction concept was also included in the work by Horii and Nemat-Nasser (1985). Their formulation for the void–void interaction problem is quite general and is applicable to a nonsymmetric structure containing voids of different sizes and subject to various boundary conditions. Also, a three-dimensional void–void interaction was studied by Rodin and Hwang (1991).

This paper presents an approach to modeling a general system containing multiple interacting holes and cracks. The superposition technique is used to divide the system into a homogeneous problem (the one without holes and cracks) and two sets of subproblems, each subproblem containing either a single hole or a single crack. Modeling the holes as unknown pseudo-tractions on the hole surfaces (Horii and Nemat-Nasser, 1985) and the cracks as an unknown distribution of dislocations renders the problem a set of integral equations. For this purpose, two types of fundamental solutions are utilized, i.e. point loads acting on the surface of a hole in an infinite body and point dislocations applied to an infinite body. The resulting integral equations present Cauchy-type singularities only in the kernels associated with cracks and present no singularities in the kernels associated with holes. This feature is attributed to the delta-function nature of the fundamental solution.

The results in terms of stress intensity factors (SIFs) obtained from the present analysis are first verified against existing solutions involving holes and cracks. The amplification and retardation effects on SIFs due to interactions among various distributions of holes and cracks are then investigated. The geometries are grouped as the pattern of the hole-and-crack arrangement, relative sizes of the cracks and holes, spacings, and crack orientations. The pattern of the hole-and-crack arrangement has significant effects on the nature of the amplification or retardation. It is found that in the fractured porous elastic medium (modeled as a crack surrounded by holes), amplification or retardation can occur, depending on the relative size of the holes and cracks and the spacing between them. Very strong retardation exists as the spacing becomes small. Some optimal retardations are achieved by adjusting the geometry parameters. An array of periodical crack–hole structures is examined as a numerical example.

2. MODELING OF MUILTIPLE INTERACTING VOIDS AND CRACKS

2.1. *Problem statement*

This section concerns the formulation of integral equations for a two-dimensional system containing a finite number of nonintersecting circular voids and cracks. Specifically, consider an infinite solid containing M arbitrarily oriented cracks and N circular voids, as shown in Fig. 1. Let (x, y) be the global Cartesian coordinates. Let $R^{(j)}$ be the radius of the jth void, $(x_v^{(j)}, y_v^{(j)})$ be the coordinates of its center, $a^{(i)}$ and $\phi^{(i)}$ be the half-length of the ith crack and its orientation angle with respect to the x-axis, and $(x_c^{(i)}, y_c^{(i)})$ be the coordinates of the ith crack center. Denote the local polar coordinate system associated with the jth

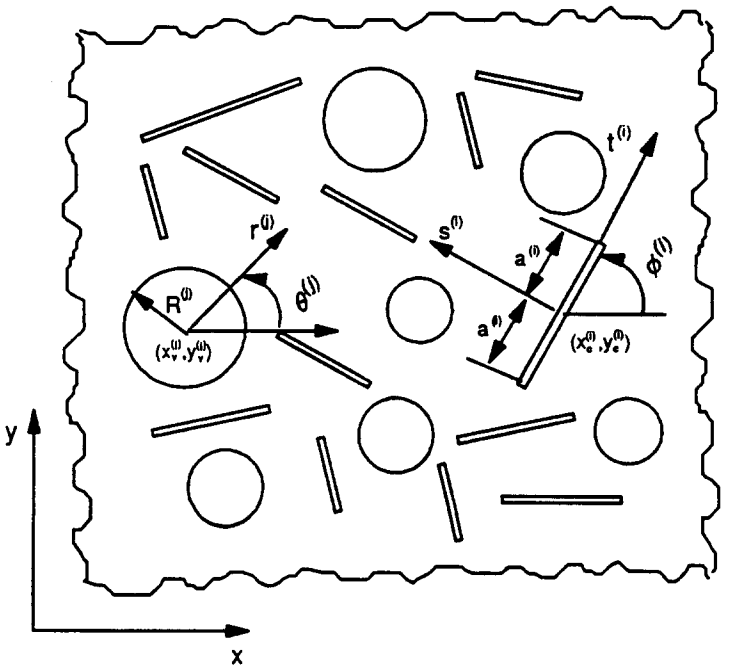

Fig. 1. Geometric description of the original problem.

void by $r^{(j)}$ and $\theta^{(j)}$, and the local coordinates normal and tangential to the ith crack by $s^{(i)}$ and $t^{(i)}$. The infinitely extended body may be subject to an arbitrary set of external loads (including quasi-static thermal loads). The boundary conditions for the surfaces of the holes and cracks are traction free (crack closure is neglected), giving

$$\sigma_{ss}^{(i)} = 0, \quad \sigma_{ts}^{(i)} = 0 \quad \text{for all cracks,} \quad i = 1, 2, \ldots, M, \tag{1}$$

$$\sigma_{rr}^{(j)} = 0, \quad \sigma_{r\theta}^{(j)} = 0 \quad \text{for all voids,} \quad j = 1, 2, \ldots, N. \tag{2}$$

We shall refer to the above-described boundary value problem as the original problem.

2.2. *Superposition*

The solution of this original problem is obtained by superposition of a homogeneous problem and a number of perturbed subproblems. In the homogeneous problem, an infinitely extended body without any voids and cracks is subjected to the same remote applied stresses as used in the original problem. The perturbed subproblems are divided into two groups. The first group consists of N subproblems associated with N holes. Each subproblem in this group concerns a single hole in an infinite body, subject to an unknown distribution of tractions on the hole surface but zero stresses at infinity. The unknown distributed tractions are called pseudo-tractions in the work by Horii and Nemat-Nasser (1985). The second group consists of M subproblems associated with M cracks. Each subproblem in this group concerns a single crack in an infinite body, subject to zero remote stresses. As in many crack problems, each single crack is modeled as an unknown distribution of dislocations along the crack line. Denote the unknown normal and tangential distributions of tractions on the jth hole by $p_r^{(j)}$ and $p_\theta^{(j)}$ and the unknown normal and tangential distributions of dislocations on the ith crack by $b_s^{(i)}$ and $b_t^{(i)}$. This decomposition of the original problem into a homogeneous problem and two groups of subproblems is illustrated in Fig. 2. The aforementioned unknown distributed tractions on each hole and dislocation densities on each crack will be determined in such a way that the traction-free conditions at all presumed locations of hole and crack surfaces are satisfied.

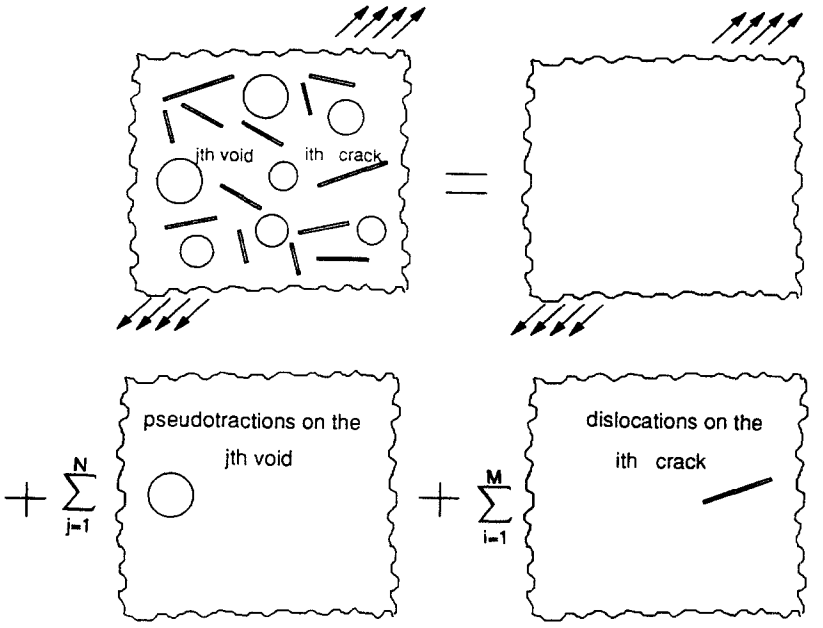

Fig. 2. Illustration of the superposition.

2.3. *Fundamental solutions*

Based on the superposition observations, two types of fundamental solutions are required for the current analysis. The first fundamental solution is for the problem of a hole in an infinite body, subject to a point force of components p_x and p_y acting at a point on the hole surface, say, $(c, 0)$, with c being the radius of the hole. The stresses at any point (x, y) are (Dundurs and Hetenyi, 1961; Hetenyi and Dundurs, 1962)

$$\sigma_{ij}^{p}(x, y; c) = \frac{1}{2\pi(1+\kappa)} H_{ijk}(x, y; c) p_k, \quad i, j, k = x, y, \tag{3}$$

where G is the shear modulus $\kappa = (3-4\nu)$ for plane strain, $\kappa = (1-\nu)/(1-2\nu)$ for generalized plane stress, and ν is the Poisson's ratio. A summation to x and y over the repeated indexes is implied.

The second fundamental solution deals with the problem of an infinitely extended body subject to a point dislocation of components (b_x, b_y) acting at a point, say, $(\xi, 0)$. The stresses at any location (x, y) can be expressed as [see, for example, Read (1953)]

$$\sigma_{ij}^{b}(x, y; \xi) = \frac{1}{\pi(1+\kappa)G} I_{ijk}(x, y; \xi) b_k, \quad i, j, k = x, y. \tag{4}$$

The first fundamental solution shown in eqn (3) can also be obtained from the analysis of Muskhelishvili (1953) by reducing an ellipse to a circle and distributed tractions to a concentrated force. Alternatively, one can also derive it from the analysis of Chen (1985). The second fundamental solution for a point dislocation in an infinite body may also be derived from the complex variable approach of Cheung and Chen (1987). For completeness, details of both the fundamental solutions, H_{ijk} $(= H_{jik})$ and I_{ijk} $(= I_{jik})$, are given in the Appendix.

It is important to note that the stress fields in eqns (3) and (4) contain a singularity of the order of r as the field point approaches the source point (r being the distance between the field point and source point). Of particular interest are the limits of the following quantities, which have the nature of a Dirac-delta function (Dundurs and Markenscoff, 1989):

$$\frac{1}{2\pi(1+\kappa)} H_{xxx}(x, y; c) \to \delta(y) \quad \text{as} \quad (x-c)^2+y^2 \to 0, \tag{5a}$$

$$\frac{1}{2\pi(1+\kappa)} H_{xyy}(x, y; c) \to \delta(y) \quad \text{as} \quad (x-c)^2+y^2 \to 0. \tag{5b}$$

This feature of the fundamental solution will be used later to formulate the integral equations, avoiding any evaluation of singular integrals along the hole surfaces.

2.4. *Integral equations*

Let us now consider the effects of all cracks and holes on the mth crack. For consistency, the stress fields associated with different cracks and voids are transformed to the local tangential-normal $(t^{(m)}, s^{(m)})$ coordinate system for the mth crack. For example, the stress fields associated with the ith crack may be transformed as

$$\sigma_{ss}^{(m)} = \sigma_{tt}^{(i)} \sin^2 \theta^{(mi)} - 2\sigma_{ts}^{(i)} \sin \theta^{(mi)} \cos \theta^{(mi)} + \sigma_{ss} \cos^2 \theta^{(mi)}, \tag{6a}$$

$$\sigma_{ts}^{(m)} = [\sigma_{ss}^{(i)} - \sigma_{tt}^{(i)}] \sin \theta^{(mi)} \cos \theta^{(mi)} + \sigma_{ts}^{(i)} [\cos^2 \theta^{(mi)} - \sin^2 \theta^{(mi)}], \tag{6b}$$

where $\sigma_{tt}^{(i)}$, $\sigma_{ts}^{(i)}$ and $\sigma_{ss}^{(i)}$ are typical stress fields expressed in the ith crack tangential–normal coodinate system and $\theta^{(mi)}$ is the angle between axes $t^{(i)}$ and $t^{(m)}$.

The contributions of all M cracks to the stress field at the presumed location of the mth crack are now represented by their corresponding distributed dislocations. Similarly, the contributions from all N holes are represented by their corresponding distributed tractions. Summing the effects of all cracks and holes on the mth crack and imposing traction-free conditions, we get

$$\sum_{i=1}^{M} \int_{-a^{(i)}}^{a^{(i)}} [K_{11}(t^{(m)}, t^{(i)}) b_t^{(i)}(t^{(i)}) + K_{12}(t^{(m)}, t^{(i)}) b_s^{(i)}(t^{(i)})] \, \mathrm{d}t^{(i)}$$

$$+ \sum_{j=1}^{N} \int_{0}^{2\pi} [K_{13}(t^{(m)}, \theta^{(j)}) p_\theta^{(j)}(\theta^{(j)}) + K_{14}(t^{(m)}, \theta^{(j)}) p_r^{(j)}(\theta^{(j)})] R^{(j)} \, \mathrm{d}\theta^{(j)}$$

$$+ \sigma_{ss}^{(m0)}(t^{(m)}) = 0, \quad m = 1, 2, \ldots, M, \tag{7a}$$

and

$$\sum_{i=1}^{M} \int_{-a^{(i)}}^{a^{(i)}} [K_{21}(t^{(m)}, t^{(i)}) b_t^{(i)}(t^{(i)}) + K_{22}(t^{(m)}, t^{(i)}) b_s^{(i)}(t^{(i)})] \, \mathrm{d}t^{(i)}$$

$$+ \sum_{j=1}^{N} \int_{0}^{2\pi} [K_{23}(t^{(m)}, \theta^{(j)}) p_\theta^{(j)}(\theta^{(j)}) + K_{24}(t^{(m)}, \theta^{(j)}) p_r^{(j)}(\theta^{(j)})] R^{(j)} \, \mathrm{d}\theta^{(j)}$$

$$+ \sigma_{ts}^{(m0)}(t^{(m)}) = 0, \quad m = 1, 2, \ldots, M, \tag{7b}$$

where $b_t^{(i)}(t^{(i)})$ and $b_s^{(i)}(t^{(i)})$ are the unknown tangential and normal distributions of the dislocations over the ith crack, $p_\theta^{(j)}(\theta^{(j)})$ and $p_r^{(j)}(\theta^{(j)})$ are the unknown tangential and normal distributions of the tractions over the jth hole, and $\sigma_{ss}^{(m0)}$ and $\sigma_{ts}^{(m0)}$ represent the stress components at the location of the mth crack, but in the absence of all cracks and holes, i.e. the stress components resulting from the homogeneous solution. The kernels K_{11}–K_{24}, depending on H_{ijk} or I_{ijk}, can be expressed in terms of two bracketed arguments as follows:

$$K_{11}(t^{(m)}, t^{(i)}) = I_{xxx} \sin^2 \theta^{(mi)} + I_{yyx} \cos^2 \theta^{(mi)} - 2I_{xyx} \sin \theta^{(mi)} \cos \theta^{(mi)}, \tag{8a}$$

$$K_{12}(t^{(m)}, t^{(i)}) = I_{xxy} \sin^2 \theta^{(mi)} + I_{yyy} \cos^2 \theta^{(mi)} - 2I_{xyy} \sin \theta^{(mi)} \cos \theta^{(mi)}, \tag{8b}$$

$$K_{13}(t^{(m)}, \theta^{(j)}) = H_{xxy}\sin^2\theta^{(mj)} + H_{yyy}\cos^2\theta^{(mj)} - 2H_{xyy}\sin\theta^{(mj)}\cos\theta^{(mj)}, \tag{8c}$$

$$K_{14}(t^{(m)}, \theta^{(j)}) = H_{xxx}\sin^2\theta^{(mj)} + H_{yyx}\cos^2\theta^{(mj)} - 2H_{xyx}\sin\theta^{(mj)}\cos\theta^{(mj)}, \tag{8d}$$

$$K_{21}(t^{(m)}, t^{(i)}) = I_{xyx}(\cos^2\theta^{(mi)} - \sin^2\theta^{(mi)}) + (I_{yyx} - I_{xxx})\sin\theta^{(mi)}\cos\theta^{(mi)}, \tag{8e}$$

$$K_{22}(t^{(m)}, t^{(i)}) = I_{xyy}(\cos^2\theta^{(mi)} - \sin^2\theta^{(mi)}) + (I_{yyy} - I_{xxy})\sin\theta^{(mi)}\cos\theta^{(mi)}, \tag{8f}$$

$$K_{23}(t^{(m)}, t^{(j)}) = H_{xyy}(\cos^2\theta^{(mj)} - \sin^2\theta^{(mj)}) + (H_{yyy} - H_{xxy})\sin\theta^{(mj)}\cos\theta^{(mj)}, \tag{8g}$$

$$K_{24}(t^{(m)}, t^{(j)}) = H_{xyx}(\cos^2\theta^{(mj)} - \sin^2\theta^{(mj)}) + (H_{yyx} - H_{xxx})\sin\theta^{(mj)}\cos\theta^{(mj)}, \tag{8h}$$

where

$$\theta^{(mi)} = \phi^{(m)} - \phi^{(i)}, \tag{9a}$$

$$\theta^{(mj)} = \phi^{(m)} - \theta^{(j)}, \tag{9b}$$

$$I_{ijk} = I_{ijk}(x, y; \xi), \tag{10}$$

with x, y and ξ being substituted as

$$x = r_c^{(mi)}\cos(\theta_c^{(mi)} - \phi^{(i)}) + t^{(m)}\cos\theta^{(mi)}, \tag{11a}$$

$$y = r_c^{(mi)}\sin(\theta_c^{(mi)} - \phi^{(i)}) + t^{(m)}\sin\theta^{(mi)}, \tag{11b}$$

$$\xi = t^{(i)}. \tag{11c}$$

Here, $r_c^{(mi)}$ is the distance between the centers of the mth and ith cracks and $\theta_c^{(mi)}$ is the angle between the x-axis and the line connecting the centers of the mth and ith cracks. Finally,

$$H_{ijk} = H_{ijk}(x, y; c), \tag{12}$$

with x, y and c being substituted as

$$x = r_c^{(mj)}\cos(\theta_c^{(mj)} - \theta^{(j)}) + t^{(m)}\cos(\phi^{(m)} - \theta^{(j)}), \tag{13a}$$

$$y = r_c^{(mj)}\sin(\theta_c^{(mj)} - \theta^{(j)}) + t^{(m)}\sin(\phi^{(m)} - \theta^{(j)}), \tag{13b}$$

$$c = R^{(j)}. \tag{13c}$$

Here, $r_c^{(mj)}$ is the distance between the centers of the mth crack and the jth void and $\theta_c^{(mj)}$ is the angle between the x-axis and the line connecting the centers of the mth crack and the jth void.

Although eqn (8) for K_{ij} is lengthy, K_{ij} carries distinct physical meaning. For example, $K_{11}(t^{(m)}, t^{(i)})$ represents the normal stress σ_{ss} (in the local coordinate system of the mth crack) at a particular point $t^{(m)}$ on the mth crack due to the tangential component (in the local coordinate system of the ith crack) of the dislocation at a particular point $t^{(i)}$ on the ith crack. Similarly, other K_{ij}s may also be interpreted.

It should be noted that the integrals along the holes (the second term) in eqns (7a) and (7b) are regular, however, the integrals along the crack (the first term) are of Cauchy-type singularity.

The boundary conditions for the voids are considered next. We focus on the mth void. By the same reasoning as for the cracks, the effects of all cracks and voids on the mth void can be added in the integral sense. After transformation to the local polar coordinates of the mth void is performed and traction-free conditions are imposed, we get

$$-p_r^{(m)}(\theta^{(m)})+\sum_{i=1}^{M}\int_{-a^{(i)}}^{a^{(i)}}[K_{31}(\theta^{(m)},t^{(i)})b_t^{(i)}(t^{(i)})+K_{32}(\theta^{(m)},t^{(i)})b_s^{(i)}(t^{(i)})]\,\mathrm{d}t^{(i)}$$
$$+\sum_{\substack{j=1\\ j\neq m}}^{M}\int_0^{2\pi}[K_{33}(\theta^{(m)},\theta^{(j)})p_\theta^{(j)}(\theta^{(j)})+K_{34}(\theta^{(m)},\theta^{(j)})p_r^{(j)}(\theta^{(j)})]R^{(j)}\,\mathrm{d}\theta^{(j)}$$
$$+\sigma_{rr}^{(m0)}(\theta^{(m)})=0,\quad m=1,2,\ldots,N \tag{14a}$$

and

$$-p_\theta^{(m)}(\theta^{(m)})+\sum_{i=1}^{M}\int_{-a^{(i)}}^{a^{(i)}}[K_{41}(\theta^{(m)},t^{(i)})b_t^{(i)}(t^{(i)})+K_{42}(\theta^{(m)},t^{(i)})b_s^{(i)}(t^{(i)})]\,\mathrm{d}t^{(i)}$$
$$+\sum_{\substack{j=1\\ j\neq m}}^{N}\int_0^{2\pi}[K_{43}(\theta^{(m)},\theta^{(j)})p_\theta^{(j)}(\theta^{(j)})+K_{44}(\theta^{(m)},\theta^{(j)})p_r^{(j)}(\theta^{(j)})]R^{(j)}\,\mathrm{d}\theta^{(j)}$$
$$+\sigma_{r\theta}^{(m0)}(\theta^{(m)})=0,\quad m=1,2,\ldots,N, \tag{14b}$$

where the kernels K_{31} and K_{44} can be given as follows:

$$K_{31}(\theta^{(m)},t^{(i)})=I_{xxx}\cos^2\theta^{(mi)}+I_{yyx}\sin^2\theta^{(mi)}+2I_{xyx}\sin\theta^{(mi)}\cos\theta^{(mi)}, \tag{15a}$$
$$K_{32}(\theta^{(m)},t^{(i)})=I_{xxy}\cos^2\theta^{(mi)}+I_{yyy}\sin^2\theta^{(mi)}+2I_{xyy}\sin^2\theta^{(mi)}\cos\theta^{(mi)}, \tag{15b}$$
$$K_{33}(\theta^{(m)},\theta^{(j)})=H_{xxy}\cos^2\theta^{(mi)}+H_{yyy}\sin^2\theta^{(mi)}+2I_{xyy}\sin\theta^{(mj)}\cos\theta^{(mj)}, \tag{15c}$$
$$K_{34}(\theta^{(m)},\theta^{(j)})=H_{xxx}\cos^2\theta^{(mj)}+H_{yyx}\sin^2\theta^{(mj)}+2I_{xyx}\sin\theta^{(mj)}\cos\theta^{(mj)}, \tag{15d}$$
$$K_{41}(\theta^{(m)},t^{(i)})=I_{xyx}(\cos^2\theta^{(mi)}-\sin^2\theta^{(mi)})+(I_{yyx}-I_{xxx})\sin\theta^{(mi)}\cos\theta^{(mi)}, \tag{15e}$$
$$K_{42}(\theta^{(m)},t^{(i)})=I_{xyy}(\cos^2\theta^{(mi)}-\sin^2\theta^{(mi)})+(I_{yyy}-I_{xxy})\sin\theta^{(mi)}\cos\theta^{(mi)}, \tag{15f}$$
$$K_{43}(\theta^{(m)},t^{(j)})=H_{xyy}(\cos^2\theta^{(mj)}-\sin^2\theta^{(mj)})+(H_{yyy}-H_{xxy})\sin\theta^{(mj)}\cos\theta^{(mj)}, \tag{15g}$$
$$K_{44}(\theta^{(m)},t^{(j)})=H_{xyx}(\cos^2\theta^{(mj)}-\sin^2\theta^{(mj)})+(H_{yyx}-H_{xxx})\sin\theta^{(mj)}\cos\theta^{(mj)}. \tag{15h}$$

Here

$$\theta^{(mi)}=\theta^{(m)}-\phi^{(i)}, \tag{16a}$$
$$\theta^{(mj)}=\theta^{(m)}-\theta^{(j)}, \tag{16b}$$

and

$$I_{ijk}=I_{ijk}(x,y;\xi), \tag{17}$$

with x, y and ξ being substituted as

$$x=r_c^{(mi)}\cos(\theta_c^{(mi)}-\phi^{(i)})+R^{(m)}\cos(\theta^{(j)}-\phi^{(i)}), \tag{18a}$$
$$y=r_c^{(mi)}\sin(\theta_c^{(mi)}-\phi^{(i)})+R^{(m)}\sin(\theta^{(j)}-\phi^{(i)}), \tag{18b}$$
$$\xi=t^{(i)}. \tag{18c}$$

Here, $r_c^{(mi)}$ is the distance between the centers of the mth void and ith crack and $\theta_c^{(mi)}$ is the angle between the x-axis and the line connecting the centers of the mth void and ith crack. Finally,

$$H_{ijk}=H_{ijk}(x,y;c) \tag{19}$$

with x, y and c being substituted as

$$x = r_c^{(mj)} \cos(\theta_c^{(mj)} - \theta^{(j)}) + R^{(m)} \cos(\theta^{(m)} - \theta^{(j)}), \tag{20a}$$

$$y = r_c^{(mj)} \sin(\theta_c^{(mj)} - \theta^{(j)}) + R^{(m)} \sin(\theta^{(m)} - \theta^{(j)}), \tag{20b}$$

$$c = R^{(j)}. \tag{20c}$$

Here, $r_c^{(mj)}$ is the distance between the centers of the mth and jth voids and $\theta_c^{(mj)}$ is the angle between the x-axis and the line connecting the centers of the mth and jth voids.

In deriving integral eqns (14a) and (14b), the Dirac-delta function nature of the fundamental solution [eqns (5a) and (5b)] is used. It is noted that the integrals in eqns (14a) and (14b) do not involve any singular part due to the use of this nature of the fundamental solution.

2.5. *Side conditions*

The side conditions rendering the problem determinate are required. The single-valuedness condition of the displacement vector requires that the dislocation density functions along each crack satisfy the following relations:

$$\int_{-a^{(i)}}^{a^{(i)}} b_t^{(i)}(t^{(i)})\, dt^{(i)} = 0, \quad i = 1, 2, \ldots, M, \tag{21a}$$

$$\int_{-a^{(i)}}^{a^{(i)}} b_x^{(i)}(t^{(i)})\, dt^{(i)} = 0, \quad i = 1, 2, \ldots, M. \tag{21b}$$

Horii and Nemat-Nasser (1985) also present a constrained condition that warrants the equilibrium state for the pseudo-tractions on each hole. Such a condition in the current analysis is automatically satisfied implicitly in eqns (14a) and (14b). To illustrate this, multiply eqn (15a) by $R^{(m)} \cos\theta^{(m)}$ and eqn (15b) by $R^{(m)} \sin\theta^{(m)}$, integrate over the mth hole, and subtract the two resulting equations. We immediately have the resultant force in the x-direction:

$$P_x = \int_0^{2\pi} [p_r^{(m)}(\theta^{(m)}) \cos\theta^{(m)} - p_\theta^{(m)}(\theta^{(m)}) \sin\theta^{(m)}]\, d\theta^{(m)} = 0 \tag{22}$$

since the integral of the other three terms over the closed contour is identically zero, via the divergence theorem (assuming no body forces).

Equations (7), (14) and (21) now provide an integral equation representation of interactions in a general system of M cracks and N voids. It is noted that the equilibrium equations of the stress state at any internal point are exactly satisfied through the nature of the two fundamental solutions. The traction-free conditions presented in eqns (7) and (14) will have to be satisfied through a numerical discretization.

2.6. *Numerical solution and stress intensity factor*

The integral equations (7) and (14) are of Cauchy-type singularity only in the kernels associated with dislocations. It is important to note that the kernels associated with hole tractions present no singularity in the integral equations, even though a singular fundamental solution is used. This advantage is attributed to the Dirac-delta function nature of the fundamental solution. The system of singular integral equations may then be solved following an effective numerical technique proposed by Erdogan *et al.* (1973). After solving these equations, all the desired field quantities, such as stresses and strains, may be evaluated by means of definite integrals with appropriate kernels. Since the main interest of this paper is in the fracture analysis, the numerical results will be presented only for the stress intensity factors. The stress intensity factors are evaluated from the solved dislocation densities following an interpolation formula given by Krenk (1975).

3. NUMERICAL RESULTS

Application of the proposed integral equation formulations to several example problems involving interactions of voids and cracks is presented in this section. The integral equation formulation can handle arbitrary distributions of cracks and holes of different sizes, along with general loading conditions, in the context of elasticity. In this section, the numerical results from the proposed integral equation formulation are first verified against existing solutions in the literature. Problems involving general systems of holes and cracks are addressed next. In particular, various geometries are investigated to show the effects of the distributions of orientation, position and size of voids and cracks on the stress intensity factors. The implications of void–crack interactions for the amplification and retardation of the stress intensity factor are examined. The numerical results show that in the fractured porous elastic medium (modeled as a crack surrounded by holes), amplification or retardation can occur, depending on the geometry. Stress retardations at the crack tips prevail when a crack is in close proximity to voids (this retardation is, of course, at the price of high-stress concentrations in the neighborhood of voids). A good retardation can also be achieved by varying the relative positions of cracks and holes. These observations have important applications to underground excavations, where the proper layout of underground workings can be used to control the propagation of pre-existing cracks in rock masses.

In the following presentation, the reported stress intensity factors (SIFs) are always normalized with respect to those of a single crack in an infinite plane subject to physical loading.

An infinite plane with a crack aligned along the center of a hole, subject to a remote tensile stress perpendicular to the crack is considered in Fig. 3. Assuming the radius of the hole is equal to the half-length of the crack ($R = a$), the SIF dependence on t/a (t is the separation between the hole and crack) agrees very well with those obtained by Isida (1973). It should be noted that perturbation of SIFs due to the hole becomes very small when the separation becomes greater than the crack length ($t/a > 2$).

Figure 4 shows two circular voids of radius R ($R/a = 1$) spaced apart by a crack of length $2a$ perpendicular to the centerline of the holes, subject to uniaxial tension. The retarded SIF variation with the separation t/a is verified against those obtained by Newman (1969). Contrary to what is observed in Fig. 3, significant retardation in normalized SIFs to 0.66 is seen when the separation is equal to $2a$. Therefore, one should be cautious about drawing a borderline beyond which the interaction can be neglected to the calculation of a certain geometry.

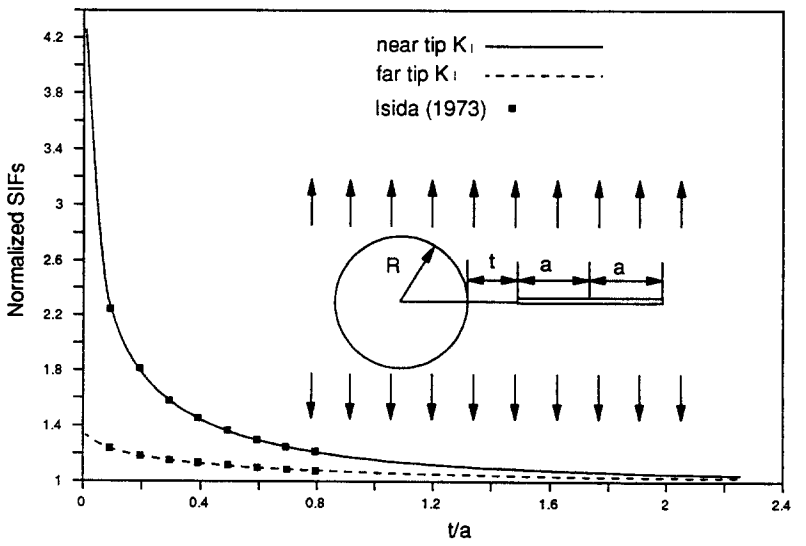

Fig. 3. Variation of the normalized SIFs of a crack aligned along the center of a hole with the separation, t/a, of the crack tip and the hole.

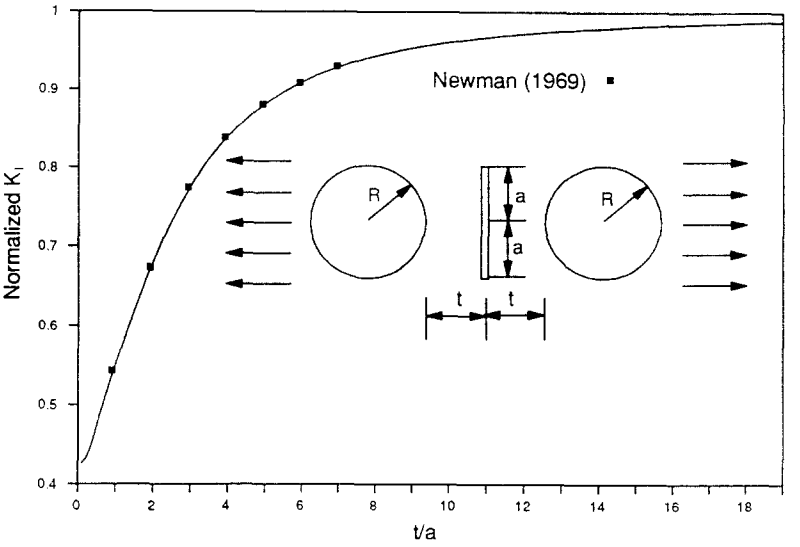

Fig. 4. Variation of the normalized SIFs of a crack perpendicular to the centerline of two holes with the separation, t/a, of the crack tip and the hole.

Figure 5(a) shows an infinite plane with a hole and a crack subject to a far-field tension perpendicular to the line connecting the centers of the hole and crack. We take the case where $R = a$ and $d = 2.2a$. Figure 5(b) shows that the variation of SIFs with the crack orientation is significantly modifed due to hole–crack interaction when compared to the case of an infinite plane with only a single crack. The near-tip and far-tip Mode-II SIFs are relatively stable for crack orientation angle α between 20° and 60°. The Mode-I SIFs change from maxima of 2.19 and 1.22 to 0.2 and 0.2, respectively, at far and near tips as the crack changes from the horizontal ($\alpha = 0°$) to the vertical ($\alpha = 90°$) position. It is noted that the nonzero value of the SIF at $\alpha = 90°$ is entirely due to the void–crack interaction.

The inset in Fig. 6 shows an infinite plane with a crack parallel between two holes, subject to a far-field tension perpendicular to the crack. We take the case where $R = a$ and $d = 1.4a$. The variation of SIFs with the distance between the center of the crack and the line connecting the centers of the holes is shown in Fig. 6. The near-tip Mode-I SIF decreases from 0.45 to a minimum value of 0.14 as t/a moves up from 0 to $0.5a$. After that, it increases to a maximum value of 1.32 at $t = 2.5a$, then starts to decay to 1.0, where there is no hole–crack interaction. The far-tip Mode-I SIF varies differently. It increases from 0.45 to a maximum value of 1.32 as t/a increases from 0 to 1.50, and then starts to decay to the stable value in a fashion similar to the near-tip SIF.

The inset in Fig. 7 shows an infinite plane with two unequal holes and a crack aligned along the centers of the holes, subject to a far-field tension. We take the case where $R_1 = a$ and $t = 0.2a$. The variation of Mode-I SIFs for two tips with the size of the hole (R_2/a) is shown in Fig. 7. The right-hand-tip Mode-I SIF increases nonlinearly as the hole size becomes bigger (the stress intensity factor changes from 1.23 to 3.45 as R_2/a increases from 0.1a to 6a). The left-hand-tip Mode-I SIF, however, increases almost linearly as the hole size increases (the stress intensity factor changes from 1.79 to 3.3 as R_2/a increases from 0.1a to 6a).

The inset in Fig. 8 shows four symmetrically distributed holes surrounding a crack subject to a field tension. We take the case where $R/a = 1$ and $d/a = 3$. The variation of Mode-I and -II SIFs with the crack orientation angle α is shown in Fig. 8. At $\alpha = 0$, the horizontally aligned holes tend to amplify the Mode-I SIF, while the vertically aligned holes tend to retard the SIF. For the chosen geometrical parameters, retardation prevails, giving a Mode-I SIF value of 0.84 at $\alpha = 0°$. The Mode-I SIF decays from 0.84 to 0.36 as the crack rotates from the horizontal position ($\alpha = 0°$) to the angle $\alpha = 67°$. The Mode-I SIF assumes a stable value of about 0.36 as the orientation angle α changes from $\alpha = 67°$ to the

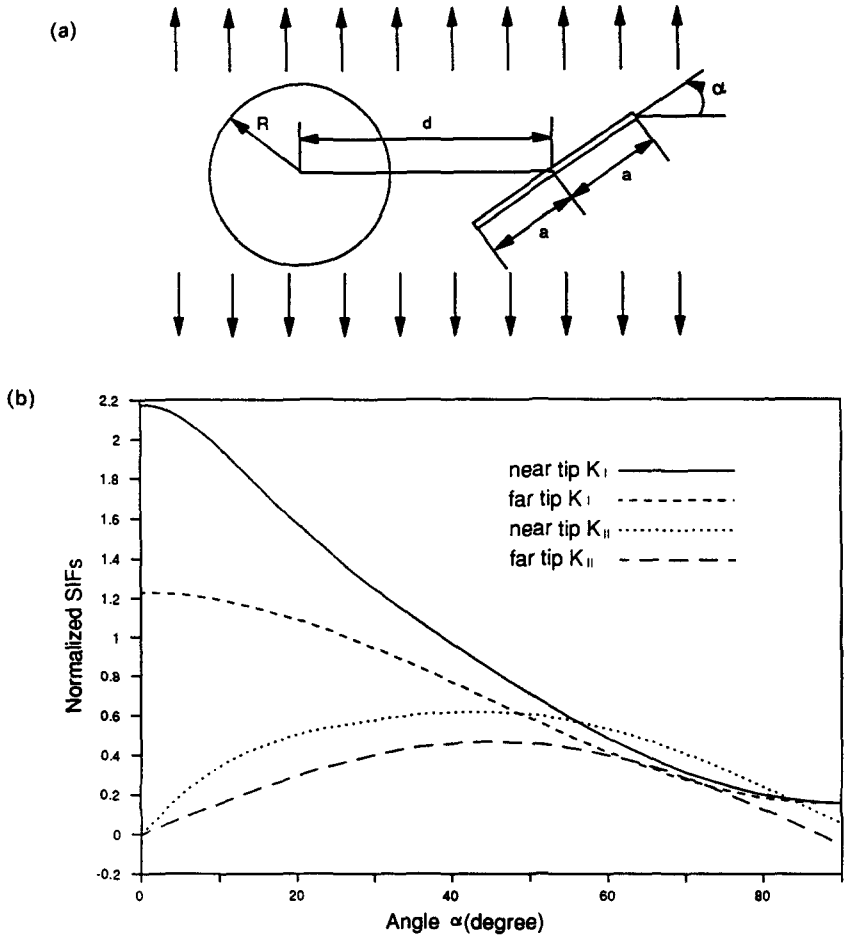

Fig. 5. A hole and an inclined crack subject to far-field tension : (a) schematic diagram ; (b) variation of SIFs with crack orientation.

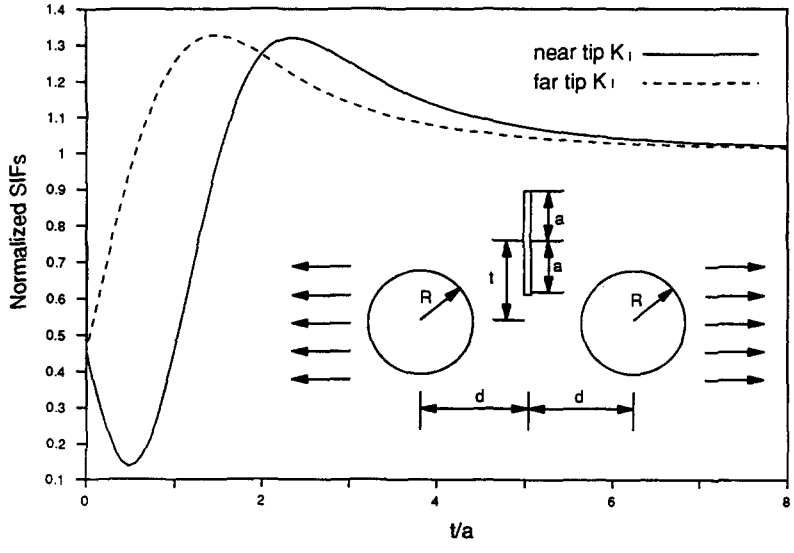

Fig. 6. Variation of SIFs with distance between center of the crack and centerline of the holes for a crack parallel between two holes.

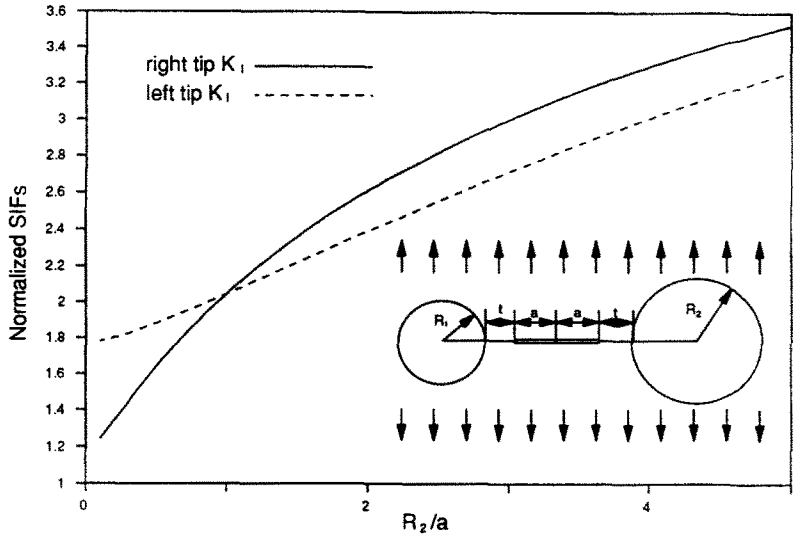

Fig. 7. Variation of SIFs with size of the hole for a crack between two unequal holes.

vertical position ($\alpha = 90°$). The Mode-II SIF increases from 0 at the horizontal position ($\alpha = 0°$) to a maximum value of 0.19 at $\alpha = 37°$ and then reverses to 0 at $\alpha = 90°$.

A further example of a crack surrounded by a square array of holes is shown in Fig. 9. This configuration can be regarded as an approximate model of a fractured porous medium. The normalized Mode-I SIF can be expressed in terms of two nondimensional parameters λ and δ, i.e.

$$K_I = F(\lambda, \delta),$$

where

$$\lambda = \frac{d}{R} \quad \text{and} \quad \delta = \frac{a}{d-R}.$$

The numercial values of the function $F(\lambda, \delta)$ for various combinations of λ and δ are given in Table 1. The results show that the smaller values of λ and δ facilitate the retardation while greater values of λ and δ favor amplification. Both of them are the results of stronger

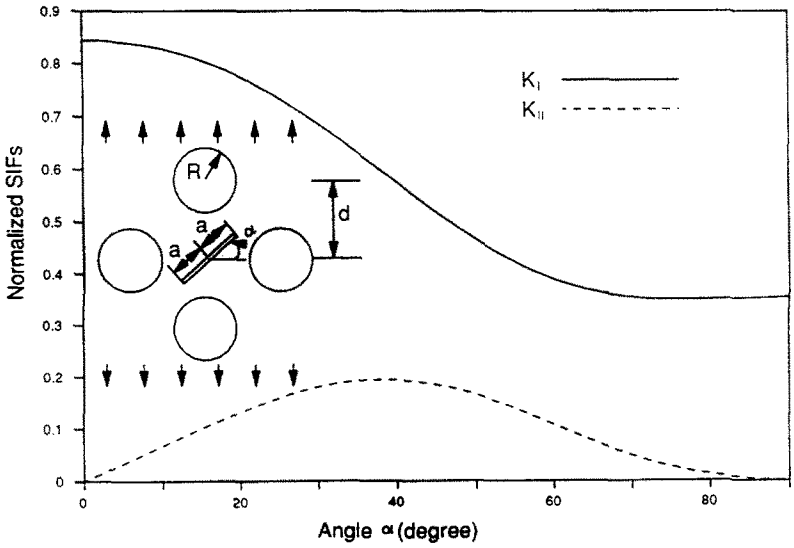

Fig. 8. Variation of SIFs with crack orientation for a crack surrounded by four symmetrically distributed holes.

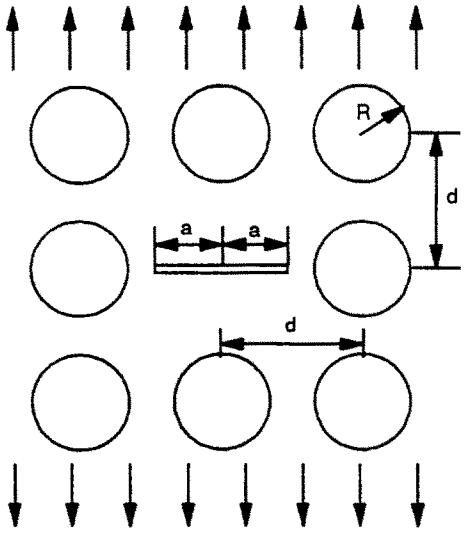

Fig. 9. Schematic diagram of a crack surrounded by a square array of holes.

interactions. It should be noted that either retardation or amplification can occur, depending on the relative size of the holes and cracks and the spacing between them. For a fixed value of λ ($\lambda > 0.4$), a certain δ yields the maximum Mode-I SIF. For example, $\delta = 4$ gives the maximum SIF value of 1.138 for $\lambda = 0.7$. The retardation is very strong as the spacing becomes small. The near-zero value of the SIF is observed for $\delta = 2$ and $\lambda < 0.5$. We have not been able to obtain convergent results for $\delta = -2$ and $\lambda \leqslant 0.3$ at 150 integral points on the crack.

Finally, an infinite body containing a row of periodic collinear crack–hole structures is considered in Fig. 10(a). The cracks are of equal size $2a$, holes are of equal radius R, and crack–hole spacing is d. The plane is subject to a uniform far-field tension. The normalized stress intensity factor can be expressed as

$$K_I = F(\lambda, \delta, M),$$

where M is the number (odd) of the cracks and

$$\lambda = \frac{d}{R}, \quad \delta = \frac{a}{d-R}.$$

The variations of Mode-I SIFs of the central crack with the parameter δ are shown in Figs 10(b), (c) and (d), for different spacing values, $\lambda = 2$, 1 and 1/2, respectively. As

Table 1. Normalized SIFs for a crack surrounded by a square array of holes

	δ				
λ	2	3	4	6	10
0.1	—	0.668	0.849	0.943	0.981
0.2	—	0.702	0.872	0.955	0.986
0.3	—	0.755	0.908	0.974	0.994
0.4	0.027	0.825	0.953	0.996	1.002
0.5	0.069	0.910	1.004	1.020	1.011
0.6	0.126	1.010	1.063	1.047	1.021
0.7	0.203	1.135	1.138	1.082	1.035
0.8	0.315	1.320	1.256	1.146	1.064
0.9	0.528	1.697	1.526	1.322	1.161

expected, the stress intensity factors increase when the spacing becomes small and the hole becomes bigger. The sensitivity of the Mode-I SIFs of the central crack to the number of cracks, M, is pronounced only for the smaller values of M. As M becomes larger, discrepancies in the SIFs of the central crack become very small for increasing values of M, and the case for an infinite series of periodical collinear hole–crack structures can be recovered. The numerical results show that $M = 11$ is sufficient to obtain the stable SIF values for the infinite series of the periodical collinear hole–crack structures with an error of less than 3%.

4. CONCLUSIONS

An integral equation approach to modeling interactions among voids (or holes) and cracks in the context of two-dimensional elastic fracture mechanics has been developed, based on two types of fundamental solutions, one due to point loads in a solid with a hole and the other due to point dislocations in an infinite elastic body. The proposed technique is capable of handling general loading conditions and arbitrary distributions of voids and cracks. The appropriate three-dimensional fundamental solutions would, of course, be required for extensions to three-dimensional problems.

The proposed integral equation approach was first verified against several existing solutions. Various distributions of voids and cracks were considered next to investigate the effects of void–crack arrangements, relative sizes of voids and cracks, spacings, and crack orientations on stress amplification and retardation. The present study reveals that very strong retardation (void toughening) exists in elastic porous media if the voids and cracks are close enough. Some optimal retardation is also achieved by adjusting the void–crack geometry parameters.

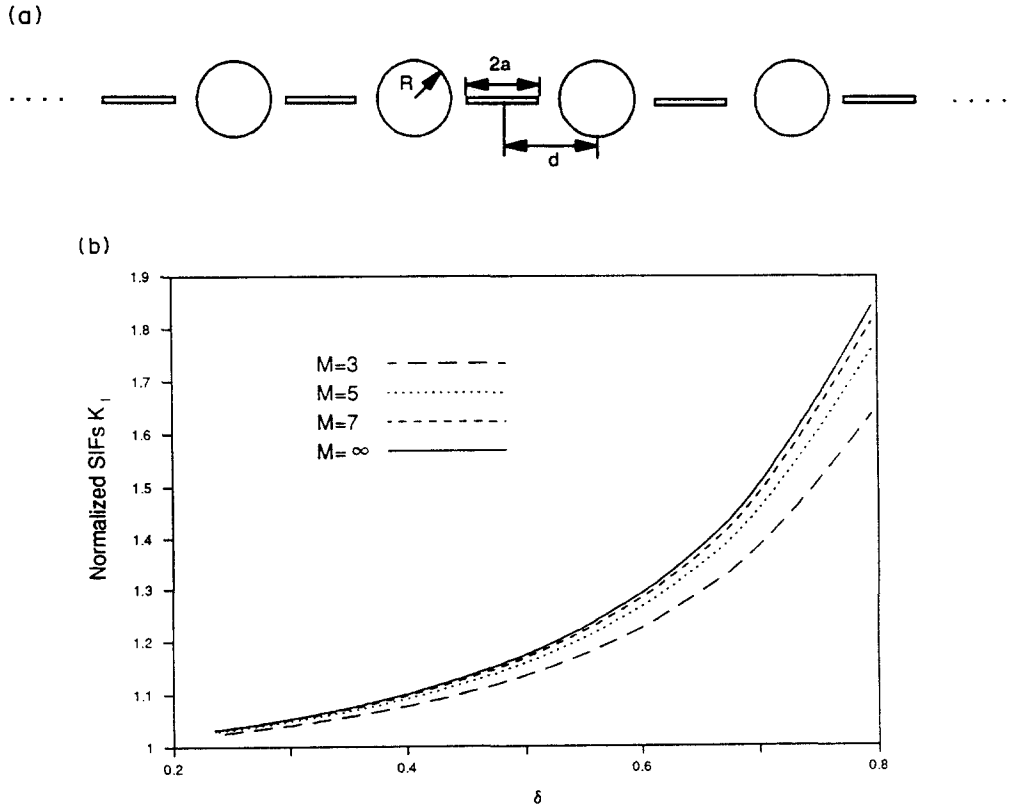

Fig. 10. A row of periodic collinear crack-hole structures: (a) schematic diagram; (b) variation of the central crack SIFs with parameter δ: $\lambda = 2$; (c) variation of the central crack SIFs with parameter δ: $\lambda = 1$; (d) variation of the central crack SIFs with parameter δ: $\lambda = 1/2$.

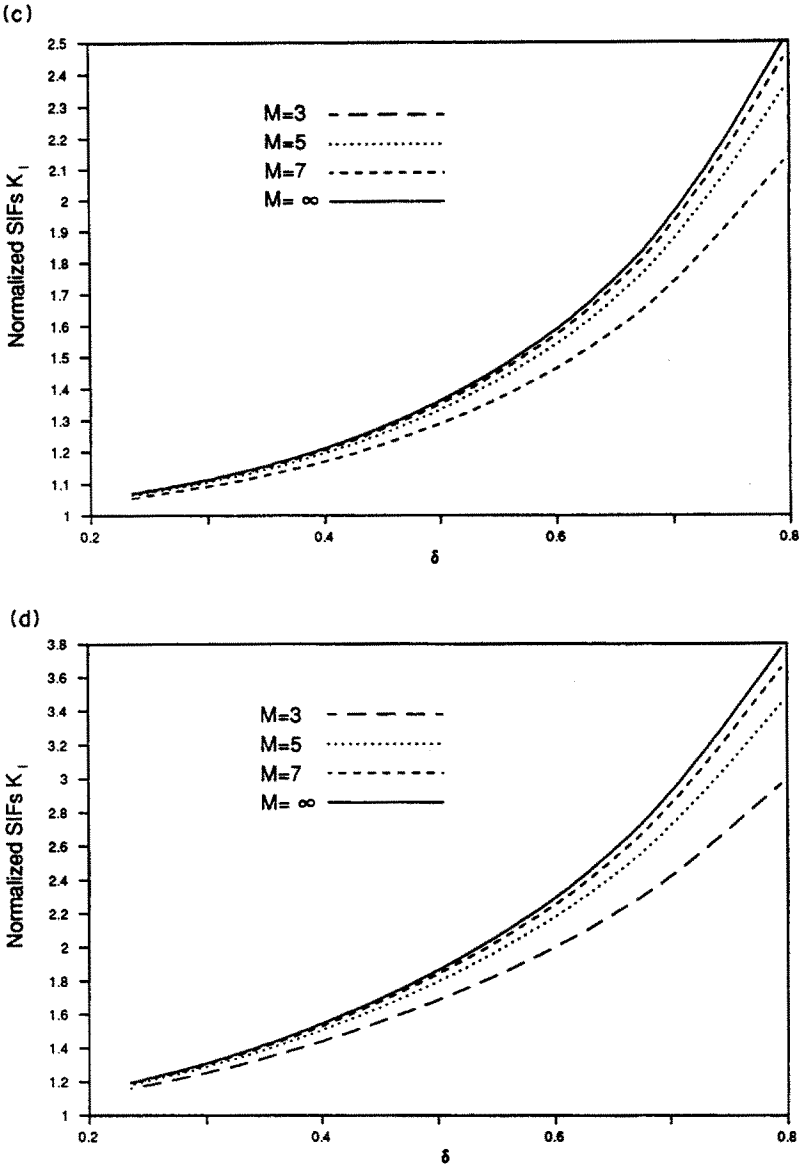

Fig. 10 (*continued*)

Many real-life materials contain a number of defects in the form of voids and cracks. Several micromechanical models have been proposed to obtain the overall behavior of such materials. The integral equation proposed here provides an avenue for numerical verification of those micromechanical models. Work on this and on enhancing numerical efficiency is currently in progress at The University of Arizona.

Acknowledgements—The authors gratefully acknowledge the financial support provided by the U.S. National Science Foundation through Grant No. DMC8657345 and by the Hughes Aircraft Company.

REFERENCES

Atkinson, C. (1972). The interaction between a crack and an inclusion. *Int. J. Engng Sci.* **10**, 127–136.

Bowie, O. L. (1956). Analysis of an infinite plate containing radial cracks originating at the boundaries of an internal circular hole. *J. Math. Phys.* **35**, 60–71.

Budiansky, B., Hutchinson, J. W. and Lambropolous, J. C. (1983). Continuum theory of dilatant transformation toughening in ceramics. *Int. J. Solids Structures* **19**, 337–355.

Budiansky, B. and O'Connell, R. J. (1976). Elastic moduli of a cracked solid. *Int. J. Solids Structures* **12**, 81–97.

Chen, Y. Z. (1984a). General case of multiple crack problems in an infinite plate. *Engng Fract. Mech.* **20,** 591–597.

Chen, Y. Z. (1984b). Solutions of multiple crack problems of a circular plate or an infinite plate containing a circular hole by using Fredholm integral equation approach. *Int. J. Fract.* **25,** 155–168.

Chen, Y. Z. (1985). A special boundary-element formulation for multiple-circular-hole problems in an infinite plate. *Comput. Meth. Appl. Mech. Engng* **50,** 263–273.

Cheung, Y. K. and Chen, Y. Z. (1987). Solutions of branch crack problems in plane elasticity by using a new integral equation approach. *Engng Fract. Mech.* **28,** 31–41.

Chudnovsky, A., Dolgopolsky, A. and Kachanov, M. (1987a). Elastic interaction of a crack with a microcrack array—I. Formulation of the problem and general form of the solution. *Int. J. Solids Structures* **23,** 1–10.

Chudnovsky, A., Dolgopolsky, A. and Kachanov, M. (1987b). Elastic interaction of a crack with a microcrack array—II. Elastic solution for two crack configurations (piece-wise constant and linear approximations). *Int. J. Solids Structures* **23,** 11–21.

Dundurs, J. and Hetenyi, M. (1961). The elastic plane with a circular insert, loaded by a radial force. *J. Appl. Mech.* **28,** 103–111.

Dundurs, J. and Markenscoff, X. (1989). A Green's function formulation of anticracks and their interaction with load induced singularities. *J. Appl. Mech.* **56,** 550–555.

Erdogan, F., Gupta, G. D. and Cook, T. S. (1973). Numerical solution of singular integral equations. In *Methods of Analysis and Solutions of Crack Problems* (Edited by G. C. Sih), pp. 386–425. Noordhoff, Leyden, The Netherlands.

Erdogan, F., Gupta, G. D. and Ratwani, M. (1974). Interaction between a circular inclusion and an arbitrary oriented crack. *J. Appl. Mech.* **41,** 1007–1013.

Fredrich, J. T., Evans, B. and Wong, T.-F. (1989). Micromechanics of the brittle to plastic transition in Carrara marble. *J. Geophys. Res.* **94,** 4129–4145.

Hallbauer, D. K., Wagner, H. and Cook, N. G. W. (1973). Some observations concerning the microscopic and mechanical behavior of quartzite specimens in stiff, triaxial compression tests. *Int. J. Rock Mech. Sci.* **10,** 713–726.

Hetenyi, M. and Dundurs, J. (1962). The elastic plane with a circular insert, loaded by a tangentially directed force. *J. Appl. Mech.* **28,** 362–368.

Hori, M. and Nemat-Nasser, S. (1987). Interacting micro-cracks near the tip in the process zone of a macro-crack. *J. Mech. Phys. Solids* **35,** 601–629.

Horii, H. and Nemat-Nasser, S. (1983). Overall moduli of solids with microcracks: load induced anisotropy. *J. Mech. Phys. Solids* **31,** 155–171.

Horii, H. and Nemat-Nasser, S. (1985). Elastic fields of interacting inhomogeneities. *Int. J. Solids Structures* **21,** 731–745.

Hu, K. X. and Chandra, A. (1992). A fracture mechanics approach to modeling strength degradation in ceramic grinding processes. *ASME J. Engng Industry* (to appear).

Hu, K. X., Chandra, A. and Huang, Y. (1992). An orthotropic material damaged by distributed cracks. AME Report 92-29, Department of Aerospace and Mechanical Engineering, University of Arizona, Tucson.

Huang, Y., Hu, K. X. and Chandra, A. (1992). Damage evaluation of solids containing dilute inclusions and microcracks. AME Report 92-30, Department of Aerospace and Mechanical Engineering, University of Arizona, Tucson.

Isida, M. (1970a). Analysis of stress intensity factors for plates containing random array of cracks. *Bull. Japan Soc. Mech. Engng* **13,** 635–642.

Isida, M. (1970b). On the determination of stress intensity factors for some common structural problems. *Engng Fract. Mech.* **2,** 61–79.

Isida, M. (1973). Methods of Laurent series expansion for internal crack problems. In *Methods of Analysis and Solution of Crack Problems* (Edited by G. C. Shih), pp. 56–130. Noordhoff, Leyden.

Isida, M., Chen, D. H. and Nisitani, H. (1985). Plane problems of an arbitrary array of crack emanating from the edge of an elliptical hole. *Engng Fract. Mech.* **21,** 983–995.

Isida, M. and Igawa, H. (1991). Analysis of a zig-zag array of circular holes in an infinite solid under uniaxial tension. *Int. J. Solids Structures* **27,** 849–864.

Isida, M. and Nemat-Nasser, S. (1987). A unified analysis of various problems relating to circular holes with edge cracks. *Engng Fract. Mech.* **27,** 571–591.

Ju, J. W. (1991). On two-dimensional self-consistent micromechanical damage models for brittle solids. *Int. J. Solids Structures* **27,** 227–258.

Kachanov, M. (1982). A microcrack model of rock inelasticity. *Mech. Mater.* **1,** 19–41.

Kachanov, M. (1987). Elastic solids with many cracks: A simple method of analysis. *Int. J. Solids Structures* **23,** 23–43.

Kachanov, M. and Montagut, E. (1986). Interaction of a crack with certain microcrack arrays. *Engng Fract. Mech.* **25,** 635–636.

Kemeny, J. and Cook, N. G. W. (1986). Effective moduli, nonlinear deformation and strength of a cracked elastic solid. *Int. J. Rock Mech. Min. Sci.* **23,** 107–118.

Krenk, S. (1975). On the use of the interpolation polynomial for solutions of singular integral equations. *Q. Appl. Math.* **32,** 479–484.

McMeeking, R. M. and Evans, A. G. (1982). Mechanics of transformation—toughening in brittle materials. *J. Am. Ceram. Soc.* **65,** 242–247.

Muskhelishvili, N. I. (1953). *Some Basic Problems of the Mathematical Theory of Elasticity*. Noorhoff, Groningen, The Netherlands.

Newman, J. C., Jr (1969). Stress analysis of simply and multiply connected regions containing cracks by the method of boundary collocation. Master's thesis, Virginia Polytechnic Institute and State University, Blacksburg.

Read, W. T. (1953). *Dislocations in Crystals*. McGraw-Hill, New York.

Rodin, G. J. and Hwang, Y.-L. (1991). On the problem of linear elasticity for an infinite region containing a finite number of non-intersecting spherical inhomogeneities. *Int. J. Solids Structures* **27,** 145–159.

Rubinstein, A. A. (1986). Macrocrack–microdefect interaction. *J. Appl. Mech.* **53,** 505–510.
Rubinstein, A. A. (1990). Crack-path effect on material toughness. *J. Appl. Mech.* **57,** 97–103.
Sih, G. C. (1973). *Handbook on Stress Internsity Factors*. Lehigh University, Bethlehem, PA.
Sumarac, D. and Krajcinovic, D. (1987). A self-consistent model for microcrack-weakened solids. *Mech. Mater.* **6,** 39–52.
Tada, H., Paris, P. and Irwin, G. (1985). *The Stress Analysis of Cracks Handbook*. Paris Productions, Inc., St Louis, MO.

APPENDIX

The fundamental functions in eqns (3) and (4) are given as:

$$H_{xxx}(x,y;c) = \frac{2(1+\kappa)x^3}{r_0^4} - \frac{4(1+\kappa)x_1^3}{r_1^4} - c(1+\kappa)\left(-\frac{1}{r_0^2}+\frac{2x^2}{r_0^4}\right)+c^2\kappa\left(\frac{6x}{r_0^4}-\frac{8x^3}{r_0^6}\right)+(-1+\kappa)\left(-\frac{x}{r_0^2}+\frac{2x^3}{r_0^4}\right),$$

$$H_{xyx}(x,y;c) = -\frac{2c(1+\kappa)xy}{r_0^4} + \frac{2(1+\kappa)x^2y}{r_0^4} - \frac{4(1+\kappa)x_1^2y}{r_1^4} + c^2\kappa\left(\frac{2y}{r_0^4}-\frac{8x^2y}{r_0^6}\right)+(-1+\kappa)\left(-\frac{y}{r_0^2}+\frac{2x^2y}{r_0^4}\right),$$

$$H_{yyx}(x,y;c) = -c(1+\kappa)\left(\frac{1}{r_0^2}-\frac{2x^2}{r_0^4}\right)+c^2\kappa\left(-\frac{6x}{r_0^4}+\frac{8x^3}{r_0^6}\right)+(1+\kappa)\left(\frac{2x}{r_0^2}-\frac{2x^3}{r_0^4}\right)+(-1+\kappa)\left(\frac{3x}{r_0^2}-\frac{2x^3}{r_0^4}\right)$$
$$-2(1+\kappa)\left(\frac{2x_1}{r_1^2}-\frac{2x_1^3}{r_1^4}\right),$$

$$H_{xxy}(x,y;c) = -\frac{2c(1+\kappa)xy}{r_0^4} + \frac{2(1+\kappa)x^2y}{r_0^4} - \frac{4(1+\kappa)x_1^2y}{r_1^4} + c^2\kappa\left(\frac{2y}{r_0^4}-\frac{8x^2y}{r_0^6}\right)+(-1+\kappa)\left(\frac{y}{r_0^2}+\frac{2x^2y}{r_0^4}\right),$$

$$H_{xyy}(x,y;c) = c(1+\kappa)\left(-\frac{1}{r_0^2}+\frac{2x^2}{r_0^4}\right)+c^2\kappa\left(-\frac{6x}{r_0^4}+\frac{8x^3}{r_0^6}\right)+(-1+\kappa)\left(\frac{x}{r_0^2}-\frac{2x^3}{r_0^4}\right)-(1+\kappa)\left(-\frac{2x}{r_0^2}+\frac{2x^3}{r_0^4}\right)$$
$$+2(1+\kappa)\left(-\frac{2x_1}{r_1^2}+\frac{2x_1^3}{r_1^4}\right),$$

$$H_{yyy}(x,y;c) = \frac{2c(1+\kappa)xy}{r_0^4} + c^2\kappa\left(-\frac{2y}{r_0^4}+\frac{8x^2y}{r_0^6}\right)+(-1+\kappa)\left(\frac{y}{r_0^2}-\frac{2x^2y}{r_0^4}\right)$$
$$-(1+\kappa)\left(-\frac{2y}{r_0^2}\right)+\left(\frac{2x^2y}{r_0^4}\right)+2(1+\kappa)\left(-\frac{2y}{r_1^2}+\frac{2x_1^2y}{r_1^4}\right),$$

where $x_1 = (x-c)$, $r_0^2 = (x^2+y^2)$, and $r_1^2 = (x_1^2+y^2)$, and

$$I_{xxx}(x,y;\xi) = -2\left(\frac{y}{r_1^2}+\frac{2x_1^2y}{r_1^4}\right),$$

$$I_{xyx}(x,y;\xi) = -2\left(\frac{x_1}{r_1^2}-\frac{2x_1^3y}{r_1^4}\right),$$

$$I_{yyx}(x,y;\xi) = -2\left(\frac{y}{r_1^2}-\frac{2x_1^2y}{r_1^4}\right),$$

$$I_{xxy}(x,y;\xi) = 2\left(-\frac{x_1}{r_1^2}+\frac{2x_1^3}{r_1^4}\right),$$

$$I_{xyy}(x,y;\xi) = 2\left(-\frac{y}{r_1^2}+\frac{2x_1^2y}{r_1^4}\right),$$

$$I_{yyy}(x,y;\xi) = 2\left(\frac{3x_1}{r_1^2}-\frac{2x_1^3}{r_1^4}\right),$$

where $x_1 = (x-\xi)$ and $r_1^2 = (x_1^2+y^2)$.